Ab Initio Study of Hydrogen Cyanide Borane(1) Polymer and Its Dehydrogenated Analog

Adriana Gregušová,*,† Štefan Varga,† Ivan Černušák,‡ and Jozef Noga*,†

Institute of Inorganic Chemistry, Slovak Academy of Sciences, SK-84236 Bratislava, Slovakia, and Department of Physical Chemistry, Faculty of Science, Comenius University, SK-84215 Bratislava, Slovakia

Received: October 17, 2001; In Final Form: August 1, 2002

Electronic structure of the polymers constructed from 1-λ^2-2-azonia-1-borata-2-propyne (HCNBH) and 2-azonia-1-λ^1-borata-2-propynyl radical (HCNB) have been studied ab initio by the use of finite periodic cluster approximation within the second-order many-body perturbation theory [MBPT(2)] with the Hartree−Fock reference. Results are compared with molecular calculations of corresponding oligomers. It is shown that though oligomers can be used for initial guess of the geometry, it is not appropriate to extrapolate some basic features of the polymer band structure from the results of increasing oligomers. $(HCNB)_n$ polymer has all of the atoms in plane, which allows for conjugation of π-electrons. The band gap of ∼2.8 eV at MBPT(2) level for $(HCNB)_n$ puts this species among semiconductors, with a possibility of further improvements of its properties by doping. $(HCNBH)_n$ polymer has a nonplanar staggered structure, and it is an insulator.

1. Introduction

Nowadays, the B/C/N materials attract an increasing attention of both experimental and theoretical chemists. This interest in B/C/N hybrids has originally been stimulated by the structural similarity[1−3] between graphite and hexagonal BN. Since then, a wide variety of B/C/N based materials of nonstoichiometric, as well as stoichiometric, composition has been synthesized, for example, polymeric $(CNBH_2)_n$,[4] B, N-substituted carbon nanotubes and nanofibers,[5−10] graphitic-like plates,[3,11−14] B/C/N films,[15−18] onionlike structures, BC_2N fullerenes,[19] and BC_3N_3 grid.[20] As well, several structures have been the subject of theoretical calculations.[21−25] Review on the synthesis of B/C/N materials, their expected properties, and possible ways of application is presented, for example, in ref 13.

A concern in these materials is motivated by their intriguing physical properties, in particular, a possibility to adjust their electrical, thermal, and mechanical properties by varying the B/C/N ratio. Such flexibility can to a large extent be induced by an impact of both the electron-donating (N atoms) and electron-accepting parts (B atoms) on the electronic structure of a given material. Altering of electron-acceptor and electron-donor regions in the chain is likely to enlarge the bending of energy bands to decrease the gap between the valence and conduction band and, hence, to improve their electrical conductivity.[26,27] Moreover, considering the stability of B/C/N hybrids, boron has been known to increase the oxidation resistance of carbon-based materials.[28]

In this study, we focus on theoretical investigation of the electronic structure of two infinite linear B/C/N arrangements with the B/C/N ratio of 1:1:1, poly-1-λ^2-2-azonia-1-borata-2-propyne, $(HCNBH)_n$, and poly-2-azonia-1-λ^1-borata-2-propynyl radical, $(HCNB)_n$. They belong to the simplest models with altering donor and acceptor parts. Such polymers, among other conjugated organic polymers, may find an application in electrooptical or electronic devices (e.g., see refs 29−36). The main goal of this study has been to identify the potential of the two aforementioned polymers along this line.

The stability and electrical properties of conjugated polymer models are extremely sensitive to the extent of bond length alternation and the planarity of the polymer backbone, which supports delocalization of electrons along the chain. Increasing the bond delocalization in a planar polymer implies smaller band gap and the increase of electrical conductivity. Even small changes in geometry can often lead to significant changes in electrical conductivity. A completely delocalized system may eventually result in semiconducting or metallic properties, but simultaneously, it is destabilized by the effect of Peierls distortion.[37] For half-filled π-systems, arrangements with highly symmetrical, idealized structures do not correspond to situations of maximum bonding. Less-symmetrical deformations are more-stable because of pairing of π-electrons. To provide reliable calculations of electronic structure, it is therefore essential to employ well-stabilized geometry for the polymer repetitive units.

Semiconducting polymers could be made highly conducting after exposing to oxidizing or reducing agents. This process is referred to as "doping" in a rather misleading analogy with the doping of inorganic semiconductors. Doping in "conducting polymer terminology" is best viewed as a redox reaction. Doping requires polymers with small ionization potential or large electron affinity or both (to be easily oxidized or reduced) and π-bonded unsaturation (to ensure its stability after doping). The π-electrons are relatively easily removed or added forming a polymeric ion without much disruption of the σ-bonds that are primarily responsible for the stability of the polymer.[38]

We combine quantum-chemical molecular calculations with solid-state modeling, both being useful tools for studying π-conjugated oligomers and polymers. Besides providing a deeper insight into the electronic structure of oligomers (e.g., in terms of frontier orbitals, ionization potentials, electron affinities, excitation energies, model IR spectra, and polarizabilities), which can offer help in an interpretation of experimental findings, molecular calculations for higher oligomers can serve for realistic estimates of geometries of repetitive units in subsequent periodic structure calculations. One should not

* To whom correspondence should be addressed. E-mail addresses: uachpapp@savba.sk; uachnoga@savba.sk.
† Slovak Academy of Sciences.
‡ Comenius University.

10.1021/jp013852+ CCC: $22.00
Published on Web 09/17/2002

forget, however, that for boundary-sensitive properties, such as in some cases the molecular HOMO−LUMO gap, simple extrapolations even from large oligomer calculations can heavily fail because of the effect of terminal parts of the chain and hence provide completely misleading results. We return to this in section 3.2. On the other hand, the geometry of the central part seems to be a boundary-insensitive quantity, and geometry extrapolations from molecular calculations can be safely numerically checked.[39] Thus, combining molecular geometries with periodic structure polymer calculations of energy and other properties offers a viable way to obtain realiable results.

Calculations presented in this paper are based on our previous molecular study of linear trans-CNB oligomers.[39] In the cited work, we have investigated the effect of increasing oligomer size (from one to six monomeric units) on the geometry of its central part, π-bond delocalization, and the stability of the oligomer with respect to an "initial cracking". Using DFT-B3LYP, we showed that the bond lengths in the central part of oligomers converge rather fast with increasing oligomer size and that the geometries of the central part of tetramers, pentamers, and hexamers of $(HCNBH)_n$ and $(HCNB)_n$ are already stabilized with respect to an impact of the chain ends for both models. For higher oligomers of the $(HCNBH)_n$ series, delocalization of π-electrons along the chain is minimized because of the nonplanarity of the CNB backbone. For planar oligomers of the $(HCNB)_n$ series, bond alternation occurs along the whole chain because of an effect analogous to Peierls distortion. Oligomers of the $(HCNB)_n$ series are more stable than those of $(HCNBH)_n$, and their thermodynamic stability is comparable to the stability of oligomers of *trans*-polyacetylene.

Aforementioned BCN-type oligomers or polymers have not yet been synthesized, though, by stacking such chains, one might form two- or three-dimensional structures similar to those known and mentioned above.

2. Computational Details

Polymer calculations use a finite periodic cluster model (vide infra) and were performed by ab initio program package of Varga and Noga, FPC.[40] Because an automatic geometry optimization is not included in FPC, to obtain a reliable geometry for repetitive motif of the polymer, we performed gradient geometry optimizations for the series of oligomers of the size from one to six monomeric units. Optimizations were done at the level of HF and DFT-B3LYP methods with DZP basis set using Gaussian 98 (or Gaussian 94)[41] suite. For comparison, second-order many-body perturbation theory (MBPT-(2)) geometry optimizations have been carried out for lower oligomers, too. Details on DFT-B3LYP optimization can be found in our previous work.[39] All optimized geometries were subject to a harmonic frequency check. Full geometry details can be found elsewhere.[42] We have to stress here that, as documented by Figures 3 and 4 of ref 39, the convergence of the central part geometry (two CNB units) was rather convincing for higher oligomers ($n = 4-6$). Therefore, instead of performing an expensive full unit cell optimization, we have used the atom positions from the central parts of the optimized geometries of these oligomers in the reference computational cell geometry for our successive electron structure calculations of the polymers.

Reported energies are those corresponding to the reference computational cell for polymers. Comparable energy increments for oligomers have been calculated by subtracting the total energies of oligomers of the size of $(n - 2)$ monomeric units from the total energies of oligomers of n monomeric units. Such an approach was implied by the fact that the reference cell used for polymer calculations consists of two monomeric units, and in this manner, the impact of the chain termination of oligomers has been minimized. Total energies and the band gaps were corrected for electron correlation effects at the second-order MBPT level.

2.1. Band Structure Calculations. Polymer calculations essentially follow the standard crystal orbital scheme[43,44] (see also ref 45). The difference is in treating the many-neighbor interactions. We have adopted a finite periodic (or cyclic) cluster model, which takes into account the translational symmetry but considers only a finite number of interatomic interactions within a strictly defined region of a finite cluster. The model was first used about 30 years ago within the semiempirical theories (see refs 46 and 47 for a review), but new implementations have been reported quite recently.[48−50] A common feature of these methods is that Born−von Kármán periodic boundary condition is imposed to a finite cluster, and then there is one to one correspondence between the electronic states in direct space and band states in the reciprocal space. The model applied here is equivalent to that from ref 49 in which the (modulo) translational invariance of integrals was easy to ensure within the zero differential overlap approximation. For ab initio calculations here, we have to impose an alternative treatment. From ref 49 follows that for sufficiently large periodic clusters (~5 nm) and covalently bound systems, which we have, the results should be close to the bulk limit values.

The cluster is defined by N (N is odd) translations (here in one dimension) $\mathbf{R}_i = n_i\mathbf{a}$, with $\mathbf{a}$ being the lattice vector and $n_i = 0, ..., \pm N/2$. The (modulo)-translational invariance of two-center one-electron integrals is accomplished by a treatment described in ref 51. As a consequence, all interactions between atomic orbitals or nuclei or both that fall within half-dimension of the cluster are included. We applied the same procedure also for two-electron integrals in products of atomic orbitals for particular electrons (1 or 2) and between those products. When more than one solution for the integral value was possible due to the imposed modulo translation (the site distance equals to half-dimension of the cluster), the average was taken.

According to the model, there are again N vectors in reciprocal space, in our one-dimensional case, $\mathbf{k}_i = (n_i/N)(2\pi/a^2)\mathbf{a}$. One can apply the standard crystal orbital theory simplified by the fact that only finite N lattice and Brillouin zone summations remain for the defined $\mathbf{R}_i$'s and $\mathbf{k}_i$'s.

The MBPT(2) energy (per unit cell) correction[45] is finally also simpler to calculate

$$E_{\mathrm{N}}^{(2)} = \frac{1}{N}\sum_{I>J}^{\mathrm{occ}}\sum_{A>B}^{\mathrm{virt}} \frac{|\langle IJ||AB\rangle|^2}{\epsilon_I + \epsilon_J - \epsilon_A - \epsilon_B} \qquad (1)$$

where composite indices I, J, ... denote both spin−orbital indices (i) and the respective $\mathbf{k}$ vectors, that is, $I \equiv (i,\mathbf{k}_i)$. $\epsilon_I \equiv \epsilon_i^{\mathbf{k}_i}$ HF orbital energies, and the antisymmetrized two-electron integrals expressed in the atomic orbital basis set read

$$\langle IJ||AB\rangle = \delta_{\mathbf{k}_i+\mathbf{k}_j,\mathbf{k}_a+\mathbf{k}_b}\sum_{\alpha\beta\gamma\delta}^{M}(c_{i\alpha}^{\mathbf{k}_i}\, c_{j\beta}^{\mathbf{k}_j})^* c_{a\gamma}^{\mathbf{k}_a}\, c_{b\delta}^{\mathbf{k}_b}\sum_{\mathbf{R}_\beta\mathbf{R}_\gamma\mathbf{R}_\delta}^{N} \mathrm{e}^{i(\mathbf{k}_a\cdot\mathbf{R}_\gamma+\mathbf{k}_b\cdot\mathbf{R}_\delta-\mathbf{k}_j\cdot\mathbf{R}_\beta)}\langle\alpha\mathbf{0}\beta\mathbf{R}_\beta||\gamma\boldsymbol{R}_\gamma\delta\mathbf{R}_\delta\rangle \qquad (2)$$

where α, ... denote atomic orbitals within a cell corresponding to the translations $\mathbf{R}_\alpha$, ... M is the total number of atomic orbitals within a computational cell. The δ function in eq 2 appears because of the conservation of momenta.

The MBPT(2) band gap calculations follow the idea of expressing the correlation corrections in terms of a perturbation series of the electron affinity and the ionization potential (assuming no orbital relaxation)[52]

$$E_{\mathrm{gap}}^{(2)} = E_{\mathrm{IP}}^{(2)} - E_{\mathrm{EA}}^{(2)} \tag{3}$$

$$E_{\mathrm{IP}}^{(2)} = \frac{1}{2}\sum_{I,J}^{\mathrm{occ}}\sum_{A}^{\mathrm{virt}}\frac{|\langle IJ||AV\rangle|^2}{\epsilon_I + \epsilon_J - \epsilon_A - \epsilon_V} - \frac{1}{2}\sum_{I}^{\mathrm{occ}}\sum_{A,B}^{\mathrm{virt}}\frac{|\langle IV||AB\rangle|^2}{\epsilon_I + \epsilon_V - \epsilon_A - \epsilon_B} \tag{4}$$

$$E_{\mathrm{EA}}^{(2)} = -\frac{1}{2}\sum_{I,J}^{\mathrm{occ}}\sum_{A}^{\mathrm{virt}}\frac{|\langle IJ||AC\rangle|^2}{\epsilon_I + \epsilon_J - \epsilon_A - \epsilon_C} + \frac{1}{2}\sum_{I}^{\mathrm{occ}}\sum_{A,B}^{\mathrm{virt}}\frac{|\langle IC||AB\rangle|^2}{\epsilon_I + \epsilon_C - \epsilon_A - \epsilon_B} \tag{5}$$

In eqs 4 and 5, the composite indices *V* and *C* refer to the highest occupied and lowest virtual orbital, respectively. Notice that in the second order the formulas 4 and 5 are identical with the Toyozawa polaron model.[45,53,54] Our algorithms for both MBPT-(2) energy and band gap calculations are direct atomic orbital integrals driven.

For the purpose of FPC band gap calculations, the convergence of finite lattice summations toward the bulk limit was checked by multipole expansion of slowly decaying terms, using multipoles up to 8th order for Coulombic terms and up to 3rd order for exchange terms.[55,56] For $N = 7$, the differences with respect to the cyclic cluster model were minimal.

To describe the band structure, the Fock matrix eigenvalues and *c* coefficients were a posteriori also evaluated in additional **k** points, while the Fock matrix in direct space was taken from the periodic cluster. Besides graphical representation of band structure, such a quasi-continuous set of **k** points served for evaluation of (projected) density of states (pDOS) using reciprocal values of analytical derivatives of $\epsilon_n(\mathbf{k})$ with respect to **k**.[57]

3. Results and Discussion

We begin this section by discussing the choice of geometries that are used for repetitive units in polymer calculations. Section 3.2 is dedicated to characterization of the electronic structures of the two polymers. In section 3.2.1, we compare the energy band gaps from polymers with their oligomer HOMO−LUMO counterparts with the aim of critical assessment of a predictive power of (extrapolated) oligomer calculations used for infinite systems. More detailed insight into the energy bands in terms of projected densities of states is given in section 3.2.2.

3.1. Geometry of the Reference Cell. In general, the size of a repetitive motif—the reference cell—for periodic calculations is dictated by the translational symmetry of the chain, as well as by additional constraints, such as in our case a constraint to keep the resulting cyclic cluster a closed-shell system. Linear oligomers and polymers are rather floppy molecules; thus, the choice for their repetitive motifs is not so obvious. Various stable conformations—more or less equivalent—may differ by the length of translational vectors, that is, in size of the computational reference cell.

For instance, for hexamers of both models, the trans conformations are almost of the same stability as cis conformations. At the DFT-B3LYP/DZP level, the cis conformations were favored by 0.5 kJ/mol for $(HCNBH)_6$ and only by 0.1 kJ/mol in the case of $H(HCNB)_6H$. Differences for orbital energies were within a diminutive range of ±0.01 eV. Because the differences are negligible and we tried to simplify the polymer calculations as much as possible, we concentrate ourselves to trans conformations. In that case, the size of the reference cell is only a half of what we had to take for cis conformations. Hence, our reference computational cell comprises two HCNBH or HCNB units, respectively, for $(HCNBH)_n$ and $(HCNB)_n$ polymers.

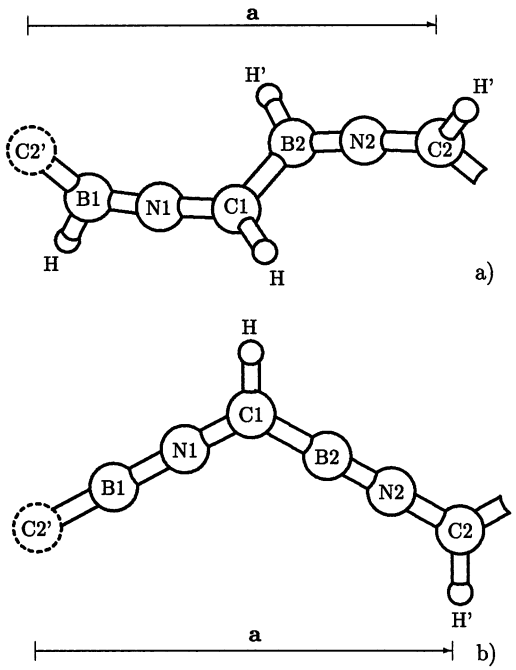

Figure 1. Reference computational cells for (a) $(HCNBH)_n$ and (b) $(HCNB)_n$ polymers.

TABLE 1: Lengths of BN, CN, and BC Bonds (in Å) of the Central Part of $(HCNBH)_n$ Oligomer Structures Optimized by Various Methods[a]

	$(HCNBH)_4$		$(HCNBH)_5$		$(HCNBH)_6$		
	HF(s)[b]	DFT(s)[c]	HF(s)[b]	DFT(s)[c]	HF(s)[b]	DFT(s)[c]	DFT(t)[c]
B1N1	1.341	1.383	1.341	1.359	1.344	1.357	1.362
B2N2	1.333	1.343	1.339	1.355	1.346	1.361	1.363
N1C1	1.248	1.251	1.249	1.264	1.248	1.265	1.264
N2C2	1.261	1.284	1.247	1.259	1.248	1.262	1.263
C1B2	1.629	1.631	1.620	1.599	1.615	1.592	1.592
C2′B1	1.590	1.544	1.621	1.600	1.618	1.601	1.594
|**a**|	7.108	7.059	7.022	7.044	7.087	7.143	7.164
symbol	GHF4s	GDF4s	GHF5s	GDF5s	GHF6s	GDF6s	GDF6t

[a] "s" and "t" denote *singlet* and *triplet* state optimized geometries, respectively. Atoms are labeled as in Figure 1. [b] DZP basis set. [c] B3LYP functional, DZP basis set.

For $(HCNBH)_n$, the reference cell is a staggered $(HCNBH)_2$ with planar (CNBHCHNB) parts (Figure 1a). For $(HCNB)_n$, the motif is planar, zigzag-shaped $(HCNB)_2$ (Figure 1b) with bond alternation along the entire chain. Geometrical parameters for these cells have been taken from the central parts of optimized oligomer structures (see section 2 and ref 39). Bond lengths from various optimizations that are interesting from the point of our discussion are summarized in Tables 1 and 2.

From our previous work,[39] we learned that the central cell energies in higher oligomers (from four to six units) were fairly stabilized. One would naturally expect that as the oligomer becomes higher, the geometry of the central cell becomes better for polymer calculations. Table 3 demonstrates that such simple correspondence may not work. We show how the energies of

TABLE 2: Lengths of BN, CN, and BC Bonds (in Å) of the Central Part of (H)(HCNB)$_n$H Oligomer Structures Optimized by Various Methods[a]

	H(HCNB)$_4$H			(HCNB)$_5$H		H(HCNB)$_6$H	
	HF(s)	DFT(s)	MP2(s)[b]	HF(s)	DFT(s)	HF(s)	DFT(s)
B1N1	1.321	1.299	1.299	1.322	1.290	1.233	1.267
B2N2	1.232	1.264	1.274	1.234	1.269	1.320	1.295
N1C1	1.251	1.295	1.307	1.251	1.298	1.371	1.342
N2C2	1.373	1.349	1.361	1.371	1.337	1.251	1.299
C1B2	1.552	1.512	1.522	1.552	1.505	1.412	1.452
C2′B1	1.409	1.441	1.445	1.411	1.458	1.553	1.508
|**a**|	7.249	7.255	7.234	7.249	7.273	7.253	7.278
symbol	GHF4s	GDF4s	GMP4s	GHF5s	GDF5s	GHF6s	GDF6s

[a] "s" and "t" denote *singlet* and *triplet* state optimized geometries, respectively. Atoms are labeled as in Figure 1. [b] Frozen core in MP2 optimization.

TABLE 3: Deviations of the Reference Cell Energies (in kJ/mol) from the Respective Apparently "Minimal" Values (E_r) for Different Geometries of Linear C/N/B Polymers

	(HCNBH)$_n$		(HCNB)$_n$	
geometry[a]	HF	MBPT(2)	HF	MBPT(2)
GDF4s	89.1	150.0	17.7	0.0
GHF4s			2.1	5.3
GMP4s			24.1	
GDF5s	0.1	0.0	23.9	4.1
GDF5s[b]	0.0	0.0		
GHF5s	2.0	12.4	2.0	6.2
GDF6s	2.7	4.0	19.4	29.6
GHF6s	1.2	11.8	0.0	54.2
GHF6s[b]	1.2	11.7		
GDF6t	2.6	1.6		
GDF6t[b]	2.5	1.5		
$-E_r/E_h$	236.391 10	237.248 59	235.164 93	236.010 35

[a] See Tables 1 and 2. All electrons correlated. [b] Symmetrized structures. Corresponding bond lengths from Table 1 were averaged.

TABLE 4: Deviations of the of Central Cell Energies[a] (in kJ/mol) for the Linear C/N/B Oligomers from the Reference Energies[b] of the Respective "Most-Stable" Polymers

		(HCNBH)$_n$	(H)(HCNB)$_n$H[c]	
n	geometry[d]	HF	HF	MBPT(2)
4	GDF	291.9	15.9	83.8
4	GHF	287.2	−1.8	100.8
5	GDF	95.8	24.7	80.7
5	GHF	82.9	0.0	101.1
6	GDF	48.6	19.6	81.0
6	GHF	47.3	−1.8	100.0

[a] $E(X_n) - E(X_{n-2})$ for X = HCNBH, HCNB; see section 2. [b] See Table 3, last row. [c] Leftmost "H" for n even only. [d] GDF ≡ GDFns,-GDF{n − 2}s; GHF ≡ GHFns,GHF{n − 2}s; see Tables 1, 2.

the reference cell vary with changing the geometries taken from different optimizations on oligomers. In Table 4, we display the differences of the oligomer "central cell energies" from the reference cell energies of the most-stable polymers. It turned out that in (HCNBH)$_n$ oligomers there was a strong quasi-degeneracy between the highest occupied and few lower virtual orbitals to such a degree that we had to skip the MBPT(2) column for (HCNBH)$_n$ in the latter table because the values were numerically inconsistent. Anyway, Table 4 demonstrates that both of the investigated polymers are more stable than corresponding oligomers.

As it is evident from Tables 1 and 3, in (HCNBH)$_n$ polymer the tendency was to stabilize structures when the two subunits were more similar. From the three closed-shell oligomers [(HCNBH)$_n$; n = 4, 6], it was the structure of the central part of pentamer for which the differences between corresponding bond lengths in the two subunits of the reference cell were the smallest. Intuitively, one would expect more symmetric conformations for even numbers of elementary units. A possible explanation for an apparent discrepancy was that in singlet state—which we optimized—the two "nonbonding" electrons originally residing on the terminal boron and carbon atoms tend to occupy a more compact molecular orbital. One would expect this orbital to be predominantly localized on either end of the oligomer backbone, which would cause certain disproportionality in the two subunits. It turned out that the electron from the terminal boron was transferred to the "carbon end side" of the oligomer, though the corresponding molecular orbital was not strictly localized at the end of the chain but delocalized along the whole terminal HBNCH unit and partially also along its neighboring HBNCH unit.

Consequently, we have expected that in triplet states the two "nonbonding" electrons could be less-influential at the center of the oligomer, because they can occupy spin−orbitals localized mostly on the two terminal units independently. Such structures for triplet states may be expected to be more stable for higher oligomers than respective singlet ground states. We have therefore performed an additional optimization for hexamer. Indeed, in the optimized structure for triplet state of (HCNBH)$_6$, the two central units, forming the reference computational cell for a polymer, are almost identical (Table 1). With respect to the singlet state, the triplet has been stabilized by 91 kJ mol^{-1}. A massive electron transfer toward the "carbon end" in singlet state is also confirmed by substantial decreasing of the dipole moment, which was 13.2 D for triplet and about 34.1 D for the singlet state.

Nevertheless, still the DFT-optimized singlet (HCNBH)$_5$ provided a slightly "better" structure for the reference cell of the polymer. Finally, symmetrizing the structures by averaging the corresponding bonds in both subunits has not changed this picture but has confirmed that the structure with fully identical HCNBH units is the most appropriate. We suppose that the pentamer singlet DFT-optimized structure is not far from the polymer optimum. As we will see in the next subsection, concerning the final conclusions small differences in geometry are not of great importance in this case.

Closer inspection of the bond lengths in Table 2 reveals that in (HCNB)$_n$ polymer a bond alternation between the two HCNB subunits is preferred. A plausible explanation for more "delocalized" bonds in (HCNB)$_5$H—or more generally in odd-membered (HCNB)$_n$H oligomers—seems to be a partial delocalization of the lone pair from the terminal carbon atom. The "best" reference cell for polymer calculations appears to be that from DFT-optimized H(HCNB)$_4$H, though one might expect the structure from a larger H(HCNB)$_6$H.

Of course, we can say that our choice for the reference cell is optimal for polymers neither at the HF level nor at the DFT-B3LYP [or MBPT(2)] level. It is, however, not necessary to rely on fully "optimized" structures for our purpose. It is known, for example, that MBPT(2) slightly overestimates the bond lengths in molecules.[58] Probably optimal HF geometries for polymer would give rise to stronger bond alternations, in accord with previous findings that HF optimizations tend to overestimate bond length alternation for *trans*-polyacetylene.[59,60]

The trends for HF vs DFT bond lengths in Table 2 lead to the same conclusions for (HCNB)$_n$ polymer. For nonplanar (HCNBH)$_n$ oligomers, such a trend has not been found (Table 1). In this case, HF optimization tends to underestimate BN

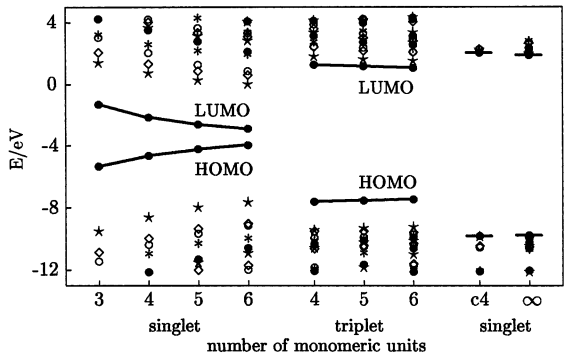

Figure 2. Orbital energies around HOMO and LUMO as functions of the oligomer size for $(HCNBH)_n$ singlet series. c4 denotes cyclic-$(HCNBH)_4$, and ∞ denotes the polymer.

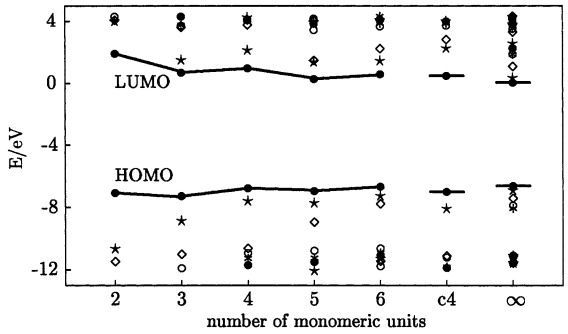

Figure 3. Singlet-state orbital energies around HOMO and LUMO as functions of the oligomer size for $(HCNB)_n$ series. c4 denotes cyclic-$(HCNB)_4$, and ∞ denotes the polymer.

and CN bond lengths and overestimate BC bond lengths as compared to the DFT-optimized parameters.

3.2. Electronic Structure. One of the important characteristics of the electronic structure that we were interested in was the band gap, in other words the gap between the highest occupied (valence) and the lowest unoccupied (conduction) bands. Directly from the cyclic cluster model, one merely obtains a discrete spectrum of crystal orbital energies for homogeneous distribution of **k** points. However, as mentioned in section 2, using the converged density matrix (in direct space), one can a posteriori evaluate the Fock matrix at any **k** point to obtain the full band structure. With the size of the cyclic cluster that we are using, the error should be negligible.[49]

3.2.1. Band Gaps. Before we come to the band structure from cyclic cluster (polymer) calculations, let us have a look at an approximate approach that is often used, namely, simulating the polymer (or solid in general) by a finite chain. Then the "band gap" is approximated by the difference between the highest occupied molecular orbital (HOMO) and the lowest unoccupied molecular orbital (LUMO), that is, by the HOMO−LUMO gap. It is believed that with increasing the cluster size one approaches the bulk limit. Results from "our" oligomers summarized in Figures 2 and 3 illustrate two different situations.

For the HCNB series, one indeed obtains HOMO−LUMO gaps that, with the size of the oligomer, more or less converge toward the polymer limit. One cannot say this even approximately for $(HCNBH)_n$ oligomers from Figure 2. Without further analysis, a series of $(HCNBH)_n$ oligomers with increasing n would apparently evoke an imagination of the bulk being a good semiconductor. In fact, the opposite is true, as can be seen from a polymer calculation.

Actually, in the previous subsection, we have mentioned the reason for such a behavior, already. HOMO and LUMO in the $(HCNBH)_n$ singlet-state oligomers are predominantly localized on the opposite ends of the oligomers. In triplet state, both of these molecular orbitals are occupied by weakly bonding electrons of equal spins and both orbitals are energetically rather close. Because of the symmetry and "closed-shell" constraints, in singlet state, the two electrons occupy a single molecular orbital (HOMO), while the latter is not as much stabilized as in triplet. Accordingly, the HOMO−LUMO gap for triplet state is, of course, larger, though still inappropriate for being a good estimate for the polymer band gap. The "terminal" electrons are "strongly bonding" in the polymer [or in the cyclic $(HCNBH)_n$]; hence, the original HOMO and LUMO levels from oligomer do not have any counterparts in a polymer.

TABLE 5: Energy Band Gaps (E_g) and Electron Affinities (EA) of Linear C/N/B Polymers (in eV) for Selected Geometries

	$(HCNBH)_n$				$(HCNB)_nH$			
	HF		MBPT(2)[b]		HF		MBPT(2)[b]	
geometry[a]	E_g	EA	E_g	EA	E_g	EA	E_g	EA
GDF4s					5.41	0.70	2.85	2.64
GHF4s					6.64	−0.02	3.94	1.96
GMP4s					5.35	0.76	2.82	2.69
GDF5s	11.64	−1.73	7.62	0.34				
GHF5s	11.65	−1.83	7.54	0.26	6.46	0.09	3.79	2.06
GDF6s	11.57	−1.69	7.50	0.38				
GHF6s	11.53	−1.73	7.52	0.32				

[a] See Tables 1,2. [b] According to eq 3, all electrons correlated.

For the HCNB oligomer series, the HOMO is a multicenter π bond along the chain. Unlike in $(HCNBH)_n$, for even numbers of HCNB units, there are no "nonbonding" electrons, and for odd numbers of HCNB units, the lone pair on the terminal carbon is fairly stabilized, with an orbital energy below the HOMO. Thus with increasing the size of the oligomer, the HOMO−LUMO gap converges to the polymer limit.

We note for completeness that for $(HCNB)_nH$ with an odd number of HCNB units the triplet state turned out to be more stable, too. Because both of the singly occupied orbitals are localized in the terminal part of carbon, the impact to the central part (i.e., our reference cell) was minimal. A singlet- vs triplet-state study for oligomers of both series will be published elsewhere.[61]

Figures 2 and 3 are illustrative, but they have resulted from a one-electron approximation. In Table 5, we have also collected values of band gaps calculated according to eqs 3−5 with inclusion of electron correlation at the MBPT(2) level. One sees that an effect of the electron correlation has been essential, indeed. With respect to Hartree−Fock results, MBPT(2) decreases the energy band gaps by 35−40%. It is known that band gaps may depend rather strongly on the actual geometry (deviations from the equilibrium geometry); therefore, we show results for several geometric arrangements.

Unlike for $(HCNB)_n$, the $(HCNBH)_n$ backbone atoms are not in a single plane; thus, a full delocalization of π-electrons is disabled. Consequently, the band gap for $(HCNBH)_n$ is larger than that for its dehydrogenated analogue. The calculated value of 7.6 eV is too large even for considering $(HCNBH)_n$ polymer as a semiconductor.

On the other hand, planarity of the polymer backbone—such as we have for $(HCNB)_n$—supports an electron delocalization leading to conjugated polymers. Full conjugation could eventually lead to a conducting system with half-filled valence band. However, in accord with Peierls,[37] the stable structure is the one with alternating bonds in the neighboring HCNB units (see Table 2). In this case, we can say that alternating are three-

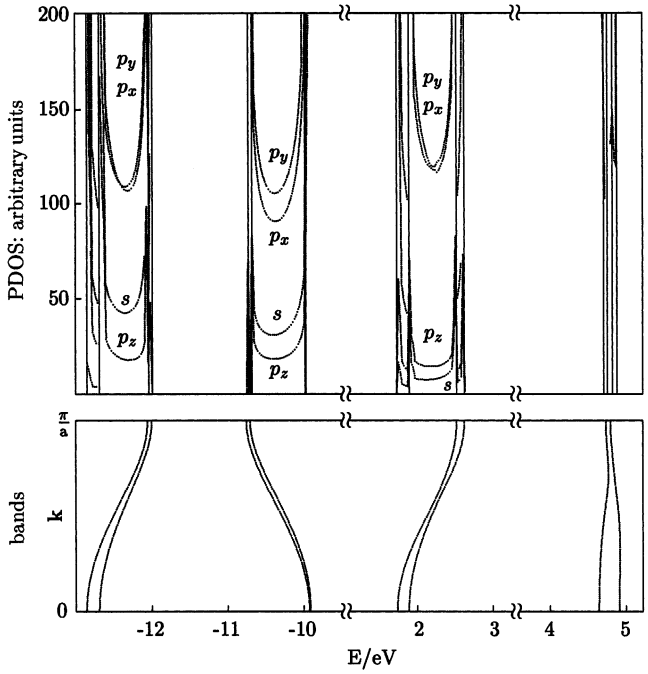

Figure 4. Band structure and projected densities of states around the valence and conduction bands for $(HCNBH)_n$ polymer.

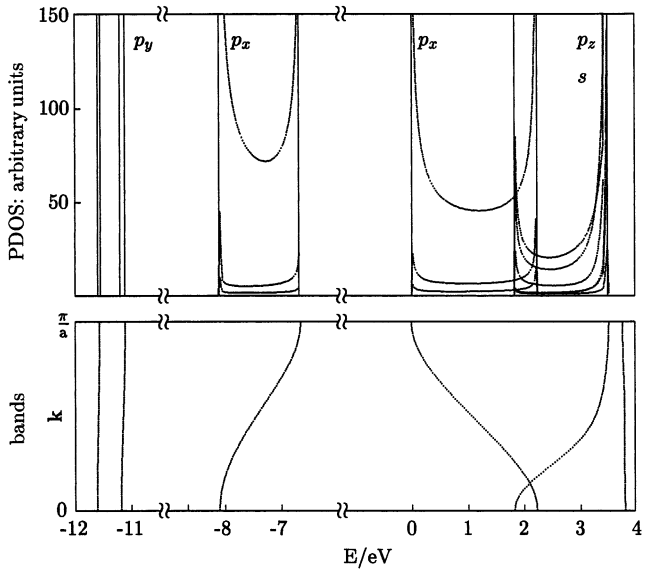

Figure 5. Band structure and projected densities of states around the valence and conduction bands for $(HCNB)_n$ polymer.

center π bonds. Such a symmetry breaking, however, gives rise to opening of the band gap. Despite that, $(HCNB)_n$ with the calculated band gap of 2.8 eV remains a potential candidate for electrooptical applications.

3.2.2. Valence and Conduction Bands. Details of electronic structure, in particular, of the valence and conduction bands, can be helpful in suggesting further adjustments of the band gap. In Figures 4 and 5, we display a few bands around the Fermi level along with projected densities of states (pDOS) for $(HCNBH)_n$ and $(HCNB)_n$, respectively.

For $(HCNBH)_n$, a direct band gap appears in the center of the Brillouin zone ($k = 0$). It is evident that the valence and conduction bands are nearly doubled. This quasi-degeneracy appears because of a symmetry in the reference cell. Though from the "rough" pDOS in the pertinent figure one sees that the dominant contributions to both valence and conduction bands come from p_x and p_y orbitals (the *z*-axis is along the direction of the translational vector), the character of bonds is not so clear. Detailed analysis reveals that the crystal orbitals are of a hybrid $\sigma-\pi$ type and even hydrogen atoms contribute significantly.

In the case of $(HCNB)_n$ (Figure 5), the direct band gap appears at the edge of the first Brillouin zone ($k = \pi/a$). Now both valence and conduction bands have a clear π-character with the major contributions from p_x of all three non-hydrogen atoms. Smaller contributions are from d_{xz} and d_{xy}. The conduction band falls almost into the region of negative energies, which implies the high electron affinity of $(HCNB)_n$. Because of these features, studies of the doping capability of this polymer can be recommended. Also, a substitution of hydrogen atoms may be of interest. To achieve a maximal effect on valence and conduction band, we propose to use a π-electron-donating substituent.

4. Conclusions

Following our study of oligomers,[39] we have investigated the electronic structure of trans conformations of two B/C/N polymers constructed from 1-λ^2-2-azonia-1-borata-2-propyne (HCNBH) and 2-azonia-1-λ^1-borata-2-propynyl radical (HCNB) as possible candidates for electrical and electrotechnical applications. Besides use of finite periodic cluster approach within Hartree−Fock approach, we have considered the effect of electron correlation within MBPT(2), both for energies and for band gaps.

The results show that $(HCNBH)_n$ with a calculated (direct) band gap of 7.6 eV is hardly expected to be of direct interest from the point of view of electrooptical materials. Contrarily, the predicted band gap of 2.8 eV for $(HCNB)_n$ is challenging. With its planar zigzag structure, bond length alternation, and electron deficiency, which are evident from the band structure, $(HCNB)_n$ is a possible candidate for electrooptical application. According to the electronic structure, we expect that the gap between the valence and conduction band can be further narrowed by doping or by substitution of the hydrogens. Both valence and conduction bands are of π-character, which predetermines the choice of the potential substituents of hydrogen atoms to π-interacting systems.

Second-order MBPT correction to total energies, and to band gaps in particular, has been essential. Inclusion of the effect of electron correlation has led to a remarkable decreasing of the band gap by 35−40% as compared with the Hartree−Fock approximation.

We also stress the risk of uncritical extrapolations of the energy band gap for the polymer from molecular calculations for a series of oligomers with increasing size because HOMO and LUMO for oligomers can be nonbonding (or weakly bonding) orbitals due to the electrons of the chain ends. Consequently, such HOMO−LUMO gaps are completely misleading.

Acknowledgment. This project was supported by the Slovak Grant Agency, VEGA (Projects 2/7203/20 and 1/7823/20). We appreciate the service of the Computer Center of the Slovak Academy of Sciences.

Supporting Information Available: Cartesian coordinates (Xmol format) for HF- and MBPT(2)-optimized oligomer geometries. This material is available free of charge via the Internet at http://pubs.acs.org.

References and Notes

(1) Badzian, A. R.; Niemyski, T.; Appenheimer, S.; Olkusnik, E. In *Proceedings of the International Conference on Chemical Vapor Deposition*; Glaski, F. A., Ed.; American Nuclear Society: Hinsdale, IL, 1972; Vol. 3.

(2) Badzian, A. R. *Mater. Res. Bull.* **1981**, *16*, 1385.
(3) Moore, A. W.; Strong, S.; Doll, G. L.; Dresselhaus, M. S.; Spain, I. L.; Bowers, C. W.; Issi, J. P.; Piraux, L. *J. Appl. Phys.* **1989**, *65*, 5109.
(4) Maya, L.; Richards, H. L. *J. Am. Ceram. Soc.* **1991**, *74*, 406.
(5) Stephan, O.; Ajayan, P. M.; Colliex, C.; Redlich, Ph.; Lambert, J. M.; Bernier, P.; Lefin, P. *Science* **1994**, *266*, 1683.
(6) Weng-Sieh, Z.; Cherrey, K.; Chopra, N. G.; Blase, X.; Miyamoto, Y.; Rubio, A.; Cohen, M.; Louie, S. G.; Zettl, A.; Gronsky, R. *Phys. Rev. B* **1995**, *51*, 11229.
(7) Zettl, A. *Adv. Mater.* **1996**, *8*, 443.
(8) Terrones, M.; Benito, A. M.; Manteca-Diego, C.; Hsu, W. K.; Osman, O. I.; Hare, J. P.; Reid, D. G.; Terrones, H.; Cheetham, A. K.; Prassides, K.; Kroto, H. W.; Walton, D. R. M. *Chem. Phys. Lett.* **1996**, *257*, 576.
(9) Suenaga, K.; Colliex, C.; Demoncy, N.; Loiseau, A.; Pascard, H.; Willaime, F. *Science* **1997**, *278*, 653.
(10) Goldgerg, D.; Bando, Y.; Han, W.; Kurashima, K.; Sato, T. *Chem. Phys. Lett.* **1999**, *308*, 337.
(11) Kouvetakis, J.; Kaner, R. B.; Sattler, M. L.; Bartlett, N. *Mater. Sci. Bull.* **1987**, *22*, 399.
(12) Kawaguchi, M.; Kawashima, T.; Nakajima, T. *Chem. Mater.* **1996**, *8*, 1197.
(13) Kawaguchi, M. *Adv. Mater.* **1997**, *9*, 615.
(14) Aoki, K.; Tanaka, S.; Tomitani, Y.; Yuda, M.; Shimada, M.; Oda, K. *Chem. Lett.* **2002**, *1*, 112−113.
(15) Saugnac, F.; Teyssandier, F.; Marchand, A. *J. Chim. Phys.* **1992**, *89*, 1453.
(16) Saugnac, F.; Teyssandier, F.; Marchand, A. *J. Am. Ceram. Soc.* **1992**, *75*, 161.
(17) Watanabe, M. O.; Itoh, S.; Mizushima, K.; Sasaki, T. *J. Appl. Phys.* **1995**, *78*, 2880.
(18) Yu, J.; Wang, E. G.; Xu, G. *Chem. Phys. Lett.* **1998**, *292*, 531.
(19) Stephan, O.; Bando, Y.; Dussarrat, C.; Kurashima, K.; Sasaki, T.; Tamiya, T. *Appl. Phys. Lett.* **1997**, *70*, 2383.
(20) Williams, D.; Pleune, B.; Kouvetakis, J.; Wiliams, M. D.; Andersen, R. A. *J. Am. Chem. Soc.* **2000**, *122*, 7735−7741.
(21) Tanaka, K.; Ueda, K.; Koike, T.; Ando, M.; Yamabe, T. *Phys. Rev. B* **1985**, *32*, 4279.
(22) Liu, A. Y.; Wentzcovitch, R. M.; Cohen, M. L. *Phys. Rev. B* **1989**, *39*, 1760.
(23) Miyamoto, Y.; Rubio, A.; Cohen, M. L.; Louie, S. G. *Phys. Rev. B* **1994**, *50*, 4976.
(24) Blase, X.; Charlier, J.-C.; De Vita, A.; Car, R. *Appl. Phys. Lett.* **1997**, *70*, 197.
(25) Boustani, I.; Quandt, A.; Hernandez, E.; Rubio, A. *J. Chem. Phys.* **1999**, *110*, 3176.
(26) Brédas, J.-L. *Adv. Mater.* **1995**, *7*, 263.
(27) Havinga, E. E.; ten Hoeve, W.; Wynberg, H. *Synth. Met.* **1993**, *55*−*57*, 299.
(28) Radovic, L. R.; Karra, M.; Skokova, K.; Thrower, P. *Carbon* **1998**, *36*, 1841.
(29) Tsumura, A.; Koezuka, H.; Ando, T. *Appl. Phys. Lett.* **1986**, *49*, 1210.
(30) Assadi, A.; Svensson, C.; Willander, M.; Inganäs, O. *Appl. Phys. Lett.* **1988**, *53*, 195.
(31) Burroughes, J. H.; Jones, C. A.; Friend, R. H. *Nature* **1988**, *335*, 137.
(32) Burroughes, J. H.; Bradley, D. D. C.; Brown, A. R.; Marks, R. N.; Mackay, K.; Friend, R. H.; Burns, P. L.; Holmes, A. B. *Nature* **1990**, *347*, 539.
(33) Burn, P. L.; Holmes, A. B.; Kraft, A.; Bradley, D. D. C.; Brown, A. R.; Friend, R. H.; Gymer, R. W. *Nature* **1992**, *356*, 47.
(34) Greenham, N. C.; Moratti, S. C., Bradley, D. D. C.; Friend, R. H.; Holmes, A. B. *Nature* **1993**, *365*, 628.
(35) Brocks, G. *J. Chem. Phys.* **1995**, *102*, 2522.
(36) Dantas, S. O.; dos Santos, M. C.; Galvão, D. S. *Chem. Phys. Lett.* **1996**, *256*, 207.
(37) Peierls, R. E. *Quantum Theory of Solids*; Oxford University Press: London, 1972.
(38) Brédas, J. L.; Street, G. B. *Acc. Chem. Res.* **1985**, *18*, 309.
(39) Pappová, A.; Černušák, I.; Urban, M.; Liebman, J. F. *J. Phys. Chem. A* **2000**, *104*, 5810.
(40) Varga, Š.; Noga, J. Program performing electronic structure calculations of finite periodic clusters (FPC), supports HF+MBPT(2) calculations of total energies and band gaps of finite clusters with explicit Born−von Karman periodic boundary conditions. 1994 (unpublished).
(41) Frisch, M. J.; Trucks, G. W.; Schlegel, H. B.; Scuseria, G. E.; Robb, M. A.; Cheeseman, J. R.; Zakrzewski, V. G.; Montgomery, J. A., Jr.; Stratmann, R. E.; Burant, J. C.; Dapprich, S.; Millam, J. M.; Daniels, A. D.; Kudin, K. N.; Strain, M. C.; Farkas, O.; Tomasi, J.; Barone, V.; Cossi, M.; Cammi, R.; Mennucci, B.; Pomelli, C.; Adamo, C.; Clifford, S.; Ochterski, J.; Petersson, G. A.; Ayala, P. Y.; Cui, Q.; Morokuma, K.; Malick, D. K.; Rabuck, A. D.; Raghavachari, K.; Foresman, J. B.; Cioslowski, J.; Ortiz, J. V.; Stefanov, B. B.; Liu, G.; Liashenko, A.; Piskorz, P.; Komaromi, I.; Gomperts, R.; Martin, R. L.; Fox, D. J.; Keith, T.; Al-Laham, M. A.; Peng, C. Y.; Nanayakkara, A.; Gonzalez, C.; Challacombe, M.; Gill, P. M. W.; Johnson, B. G.; Chen, W.; Wong, M. W.; Andres, J. L.; Head-Gordon, M.; Replogle, E. S.; Pople, J. A. *Gaussian 98*, revision A.6; Gaussian, Inc.: Pittsburgh, PA, 1998.
(42) See the Supporting Information for ref 39.
(43) Del Re, G.; Ladik, J.; Biczó, G. *Phys. Rev.* **1967**, *155*, 997.
(44) André, J.-M.; Gouverneur, L.; Leroy, G. *Int. J. Quantum Chem.* **1967**, *1*, 427, 451.
(45) Ladik, J. *Quantum Theory of Polymers as Solids*; Plenum: New York, London, 1988.
(46) Deák, P. *Phys. Status Solidi B* **2000**, *217*, 9.
(47) Evarestov, R. A.; Bredow, Th.; Jug, K. *Phys. Solid State* **2001**, *43*, 1774.
(48) Stewart, J. *J. Comput. Chem.* **1998**, *19*, 168.
(49) Noga, J.; Baòacký, P.; Biskupiè, S.; Boèa, R.; Pelikán, P.; Svrèek, M.; Zajac, A. *J. Comput. Chem.* **1999**, *20*, 253. Zajac, A.; Pelikán, P.; Noga, J.; Baòacký, P.; Biskupiè, S.; Svrèek, M. *J. Phys. Chem. B* **2000**, *104*, 1708.
(50) Bredow, T.; Geudtner, G.; Jug, K. *J. Comput. Chem.* **2001**, *22*, 89.
(51) Chandrasekhar, J.; Das, P. K. *J. Phys. Chem.* **1992**, *96*, 679.
(52) Sun, J.-Q.; Bartlett, R. J. *J. Chem. Phys.* **1996**, *104*, 8553.
(53) Toyozawa, Y. *Prog. Theor. Phys. (Kyoto)* **1954**, *12*, 422.
(54) Suhai, S. *Phys. Rev. B* **1983**, *27*, 3506.
(55) Piela, L.; Delhalle, J. *Int. J. Quantum Chem.* **1978**, *13*, 605. Delhalle, J.; Piela, L.; André, J. M. *Phys. Rev. B* **1980**, *22*, 6254.
(56) Sun, J.-Q.; Bartlett, R. J. *J. Chem. Phys.* **1997**, *106*, 5554.
(57) Delhalle, J. In *Electronic Structure of Polymers and molecular Crystals*, André, J.-M., Ladik, J., Eds.; Plenum Press: New York, London, 1975; p 53.
(58) Urban, M.; Černušák, I.; Kellõ, V.; Noga, J. In *Methods in Computational Chemistry*; Wilson, S., Ed.; Plenum Press: New York, 1987; Vol. 1, p 117.
(59) Springborg, M.; Calais, J.-L.; Goscinski, O.; Eriksson, L. A. *Phys. Rev. B* **1991**, *44*, 12713 and the references therein.
(60) Suhai, S. *Phys. Rev. B* **1995**, *51*, 16553.
(61) Gregušová, A.; Varga, Š; Černušák, I.; Noga, J., manuscript in preparation.